



Short communication

Isomorphism and solid solutions among Ag- and Au-selenides

Galina A. Palyanova^{a,b}, Yurii V. Seryotkin^{a,b}, Konstantin A. Kokh^{a,b,c,*}, Vladimir V. Bakakin^d^a Sobolev Institute of Geology and Mineralogy, Novosibirsk, Russia^b Novosibirsk State University, Russia^c Tomsk State University, Russia^d Nikolaev Institute of Inorganic Chemistry, Novosibirsk, Russia

ARTICLE INFO

Article history:

Received 16 April 2016

Received in revised form

6 June 2016

Accepted 6 June 2016

Available online 7 June 2016

Keywords:

Isomorphism

Gold

Silver

Solid solutions (Ag,Au)₂Se

Structure features

ABSTRACT

Au-Ag selenides were synthesized by heating stoichiometric mixtures of elementary substances of initial compositions $\text{Ag}_{2-x}\text{Au}_x\text{Se}$ with a step of $x=0.25$ ($0 \leq x \leq 2$) to 1050 °C and annealing at 500 °C. Scanning electron microscopy, optical microscopy, electron microprobe analysis and X-ray powder diffraction methods have been applied to study synthesized samples. Results of studies of synthesized products revealed the existence of three solid solutions with limited isomorphism $\text{Ag} \leftrightarrow \text{Au}$: naumannite $\text{Ag}_2\text{Se} - \text{Ag}_{1.94}\text{Au}_{0.06}\text{Se}$, fischesserite $\text{Ag}_3\text{AuSe}_2 - \text{Ag}_{3.2}\text{Au}_{0.8}\text{Se}_2$ and gold selenide $\text{AuSe} - \text{Au}_{0.94}\text{Ag}_{0.06}\text{Se}$. Solid solutions and AgAuSe phases were added to the phase diagram of Ag-Au-Se system. Crystal-chemical interpretation of Ag-Au isomorphism in selenides was made on the basis of structural features of fischesserite, naumannite, and AuSe.

© 2016 Elsevier Inc. All rights reserved.

1. Introduction

The low temperature selenides of silver and gold (naumannite, $\beta\text{-Ag}_2\text{Se}$; fischesserite, $\beta\text{-Ag}_3\text{AuSe}_2$) are typical minerals of noble metals in epi- and mesothermal gold deposits worldwide [1–3]. Solid solution (Ag, Au)₂Se occurs in the ores of the Ozernovskoe deposit (Kamchatka, Russia) [4]. Two polymorphs of gold selenide (α - and β -AuSe) have not been found in nature [5]. By analogy with the Ag-Au-S system [6–8], the system Ag-Au-Se may also contain the ternary compound of $\text{AgAuSe} - \text{Se}$ -analog of petrovskaitaite (AgAuS). Phase diagram of the pseudo-binary system $\text{Ag}_{2-x}\text{Au}_x\text{Se}$ was created by [9] in a narrow range of compositions $0 \leq x \leq 0.5$ at temperatures 25–960 °C. Phase relations in the Ag-Au-Se system for the interval 25–227 °C have been studied by [10,11]. The absence of the ternary compound AgAuSe in the Ag-Au-Se system was confirmed by solid-phase annealing [10]. Petrovskaitaite-like phases of AgAuSe and $\text{Ag}_{2-x}\text{Au}_x\text{Se}$ were synthesized by [12,13].

In contrast to Ag-Au-S, phase diagram Ag-Au-Se is less studied and requires further research. Phase diagrams can be used in pyrometallurgy to provide a better understanding of the process and behavior of the components during smelting and solidification. Selenides have become widely used to help assess conditions of ore formation of precious metals [3]. The aim of this work is to

study the pseudo-binary system $\text{Ag}_{2-x}\text{Au}_x\text{Se}$ $0 \leq x \leq 2$ and $\text{Ag} \leftrightarrow \text{Au}$ isomorphism in the selenides.

2. Experiments and analytical methods

2.1. Starting compositions

Experiments on the synthesis of phases of $\text{Ag}_{2-x}\text{Au}_x\text{Se}$ series ($x=0; 0.25; 0.5; 0.75; 1; 1.25; 1.5; 1.75; 2$) were performed using the procedure carried out earlier on other gold and silver sulfides and selenides AgAuS , Au_3AuSe_2 , Ag_2S , Ag_2Se [8,14,15]. Gold and silver (99.99%) as well as selenium (99.9%) with a total weight of 500 mg were taken as initial substances. Accuracy of weighing was ± 0.05 mg (“Mettler Instrument Ag CH-8606 Greifensee-Zurich”). Ampoules were heated for 3 days at a rate of 0.2–0.5°/min to 1050 °C, kept at this temperature during 12 h and then cooled at a rate of 0.2°/min to 500 °C and annealed during 3 days. After annealing, the ampoules were cooled to room temperature in the switched off furnace.

2.2. Analytical techniques

Optical microscopy, scanning electron microscopy (SEM), electron microprobe analysis (EPMA) and X-ray powder diffraction methods were applied to study synthesized substances. A polished section was prepared from synthesized phases for microscopy

* Correspondence to: IGM SB RAS, Koptyuga ave., 3, Novosibirsk 630090, Russia.
E-mail address: k.a.kokh@gmail.com (K.A. Kokh).

Table 1
The results of electron microprobe (EMPA) analysis of the solid phases crystallized in experiments with the initial composition $\text{Ag}_{2-x}\text{Au}_x\text{Se}$ (a step of $x=0.25$, $0 \leq x \leq 2$) and temperature of annealing 500 °C. N_{Au} - fineness of Au-Ag alloys in %.

N	Initial composition	Phase assemblages					
		Ag_2Se	Ag_3AuSe_2	AgAuSe	AuSe	$\text{Ag, Au } (N_{\text{Au}}, \%)$	Se
1	Ag_2Se	Ag_2Se	–	–	–	–	•
2	$\text{Ag}_{1.75}\text{Au}_{0.25}\text{Se}$	$\text{Ag}_{1.94}\text{Au}_{0.06}\text{Se}$	$\text{Ag}_{3.2}\text{Au}_{0.8}\text{Se}_2$	–	–	$\text{Au}_{0.75}\text{Ag}_{0.25}$ (850)	•
3	$\text{Ag}_{1.5}\text{Au}_{0.5}\text{Se}$	–	$\text{Ag}_{3.0}\text{Au}_{1.0}\text{Se}_{2.0}$	–	–	–	•
4	$\text{Ag}_{1.25}\text{Au}_{0.75}\text{Se}$	–	$\text{Ag}_{3.0}\text{Au}_{1.0}\text{Se}_{2.0}$	$\text{Ag}_{1.0}\text{Au}_{1.0}\text{Se}_{1.0}$	$\text{Au}_{0.94}\text{Ag}_{0.06}\text{Se}$	–	•
5	AgAuSe	–	$\text{Ag}_{3.0}\text{Au}_{1.0}\text{Se}_{2.0}$	$\text{Ag}_{1.0}\text{Au}_{1.0}\text{Se}_{1.0}$	$\text{Au}_{0.95}\text{Ag}_{0.05}\text{Se}$	$\text{Au}_{0.97}\text{Ag}_{0.03}$ (980)	•
6	$\text{Ag}_{0.75}\text{Au}_{1.25}\text{Se}$	–	$\text{Ag}_{3.0}\text{Au}_{1.0}\text{Se}_{2.0}$	$\text{Ag}_{0.98}\text{Au}_{0.98}\text{Se}_{1.04}$	$\text{Au}_{0.96}\text{Ag}_{0.04}\text{Se}$	$\text{Au}_{0.97}\text{Ag}_{0.03}$ (980)	•
7	$\text{Ag}_{0.5}\text{Au}_{1.5}\text{Se}$	–	$\text{Ag}_{3.0}\text{Au}_{1.0}\text{Se}_{2.0}$	$\text{Ag}_{1.0}\text{Au}_{1.0}\text{Se}_{1.0}$	$\text{Au}_{1.0}\text{Se}_{1.0}$	$\text{Au}_{1.0}$ (1000)	•
8	$\text{Ag}_{0.25}\text{Au}_{1.75}\text{Se}$	–	$\text{Ag}_{3.0}\text{Au}_{1.0}\text{Se}_{2.0}$	$\text{Ag}_{1.0}\text{Au}_{1.0}\text{Se}_{1.0}$	$\text{Au}_{0.95}\text{Ag}_{0.05}\text{Se}$	$\text{Au}_{0.97}\text{Ag}_{0.03}$ (980)	•
9	Au_2Se	–	–	–	–	$\text{Au}_{1.0}$ (1000)	$\text{Se}_{1.0}$

Compositions are given in molar portions, with the values exceeding the significant digits by one unit.

* Selenium was present on the walls of the ampoules in minor amounts in the form of black micro hemispheres.

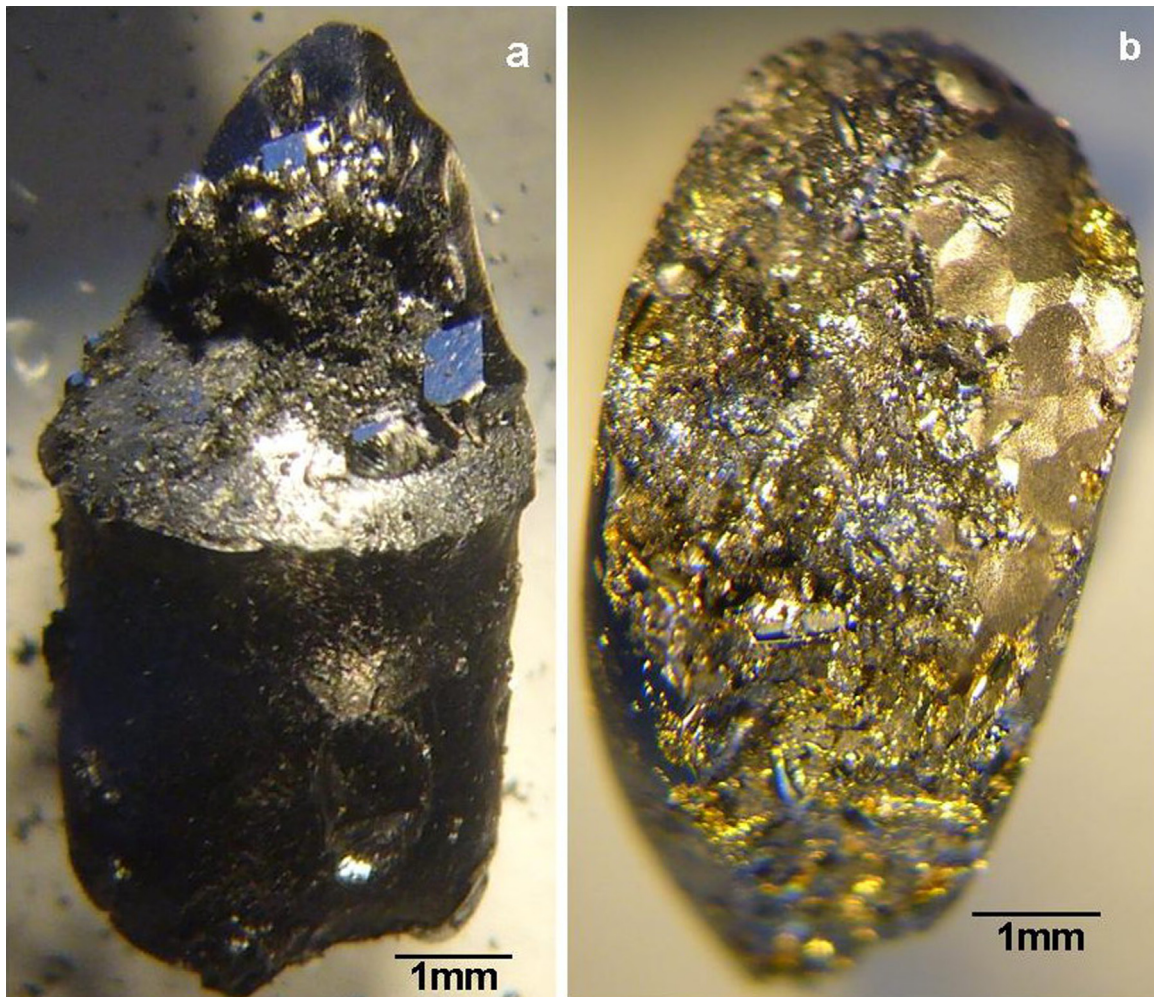


Fig. 1. Photos of synthesized homogeneous (a) and nonhomogeneous (b) samples from the experiments with the initial composition $\text{Ag}_{1.5}\text{Au}_{0.5}\text{Se}$ (a) and $\text{Ag}_{0.5}\text{Au}_{1.5}\text{Se}$ (b) (#3 and 7, Table 1).

analyses. Studies on the chemical composition of the synthesized substances were carried out using MIRA 3 LMU SEM (TESCAN Ltd.) combined with microanalysis system INCA Energy 450+ on the basis of the high sensitive silicon drift detector XMax-80, and WDS INCA Wave 500 (Oxford Instruments Ltd.). Operation conditions: accelerating voltage, 20 kV; probe current, 1.5 nA; spectrum

recording, 15 s; and spot size, 12 nm. In all measurements the electron beam was slightly defocused for reducing the effect of a sample microrelief and decreasing the destructive influence of the electron beam on unstable silver selenides. Pure silver, gold and PbSe were used as standards for Ag, Au, and Se, respectively. The analysis accuracy was 1–1.5 relative %.

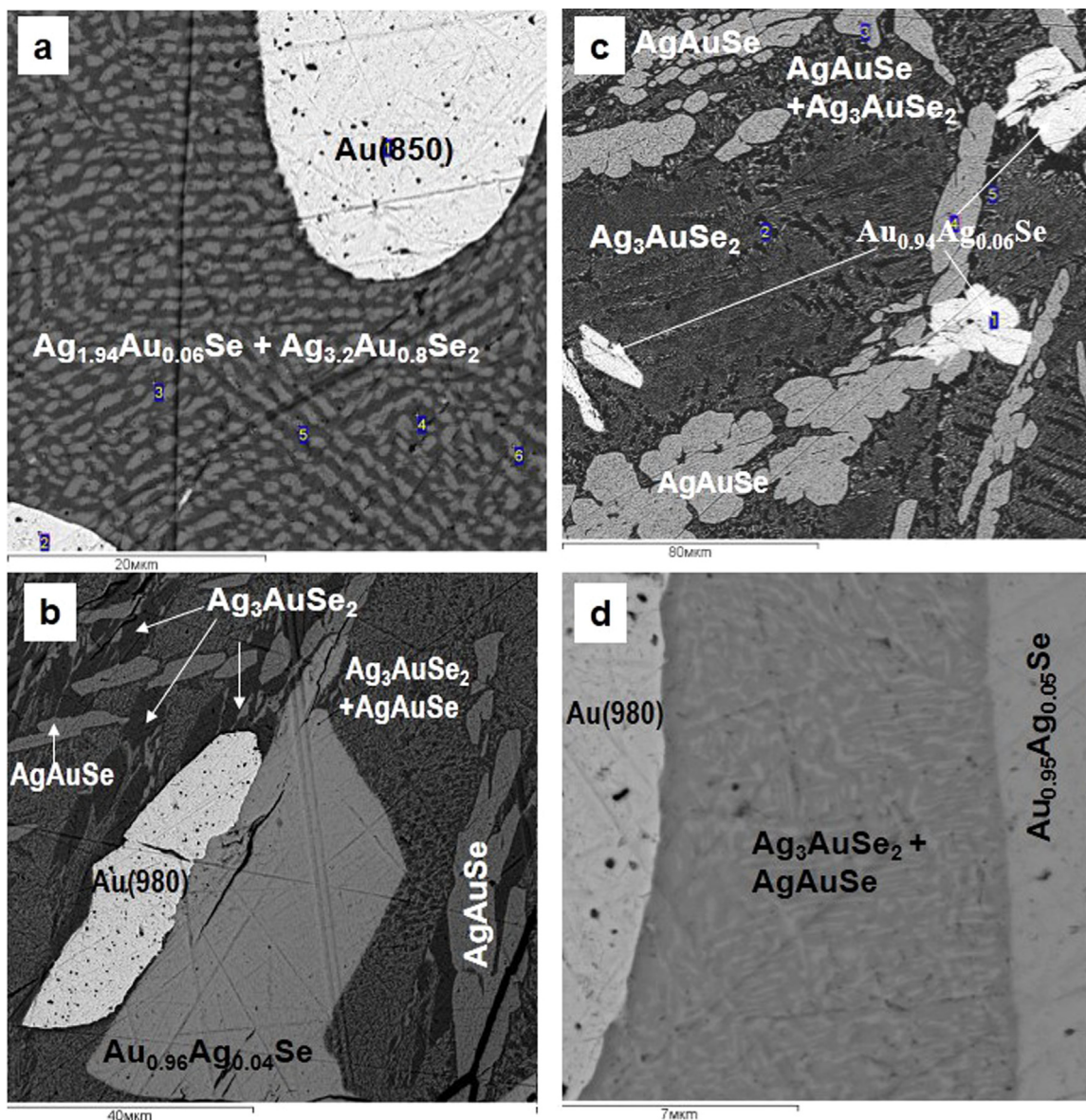


Fig. 2. SEM photos illustrating the assemblages and structures in synthesized polyphase samples with initial compositions: a) $\text{Ag}_{1.75}\text{Au}_{0.25}\text{Se}$, b) $\text{Ag}_{1.25}\text{Au}_{0.75}\text{Se}$, c) $\text{Ag}_{0.75}\text{Au}_{1.25}\text{Se}$, d) $\text{Ag}_{0.25}\text{Au}_{1.75}\text{Se}$ (#2,4,6 and 8, Table 1).

X-ray powder diffraction patterns were collected on a Stoe STADI MP diffractometer ($\text{CuK}\alpha 1$ radiation, $\text{Ge}(111)$ monochromator, 40 kV, 40 mA). Powdered silicon was used as the external standard ($a=5.4309 \text{ \AA}$). The diffraction data were collected from 5° to 60° 2θ angular range. For the phase analysis, the PDF-4 database was used. The refinement of the unit cell parameters was carried out by Rietveld method using GSAS program [16].

3. Results and discussion

Results of studies of solid-phase synthesized products with the initial predetermined compositions $\text{Ag}_{2-x}\text{Au}_x\text{Se}$ ($x=0; 0.25; 0.5; 0.75; 1; 1.25; 1.5; 1.75; 2$) are listed in Table 1. In two experiments with $x=0$ and $x=0.5$ (#1 and 3) we obtained phases that are homogeneous under optical and scanning microscopes. The compositions of these phases are identical to the predetermined initial mixtures and the structure is similar to low-temperature polymorphs: $\beta\text{-Ag}_2\text{Se}$ (naumannite) and $\beta\text{-Ag}_3\text{AuSe}_2$ (fischesserite),

respectively. As an example in Fig. 1 we showed the homogeneous ingot from experiment #3 ($\text{Ag}_{1.5}\text{Au}_{0.5}\text{Se}$) and the polyphase ingot from experiment #7 ($\text{Ag}_{0.5}\text{Au}_{1.5}\text{Se}$). Experimental products with $x=2$ (without silver) contain elementary gold and selenium, the same as the initial loading charge (#9, Table 1). Selenium forms roundly shaped grains in gold, whereas other selenium grains contain microinclusions of gold, which evidences the existence of two melts in the Au-Se system. The contents of gold in selenium and selenium in gold seem to be below the detection limit of microprobe analysis. Neither AuSe, nor Au_2Se have been detected among the newly formed phases in the synthesis products of this experiment.

At $x=0.25$ (#2, Table 1) the synthesized products were found to contain several phases: Au-bearing naumannite ($\text{Ag}_{1.94}\text{Au}_{0.06}\text{Se}$), fischesserite enriched in silver, compared to ideal stoichiometry ($\text{Ag}_{3.2}\text{Au}_{0.8}\text{Se}_2$), and high-fineness alloy 850%. The other synthesized samples (#4–8, Table 1) with initial x from 0.75 to 1.75 contained: stoichiometric fischesserite (Ag_3AuSe_2), petrovskaita-like phase AgAuSe and selenide AuSe or $\text{Au}_{0.94}\text{Ag}_{0.06}\text{Se}$,

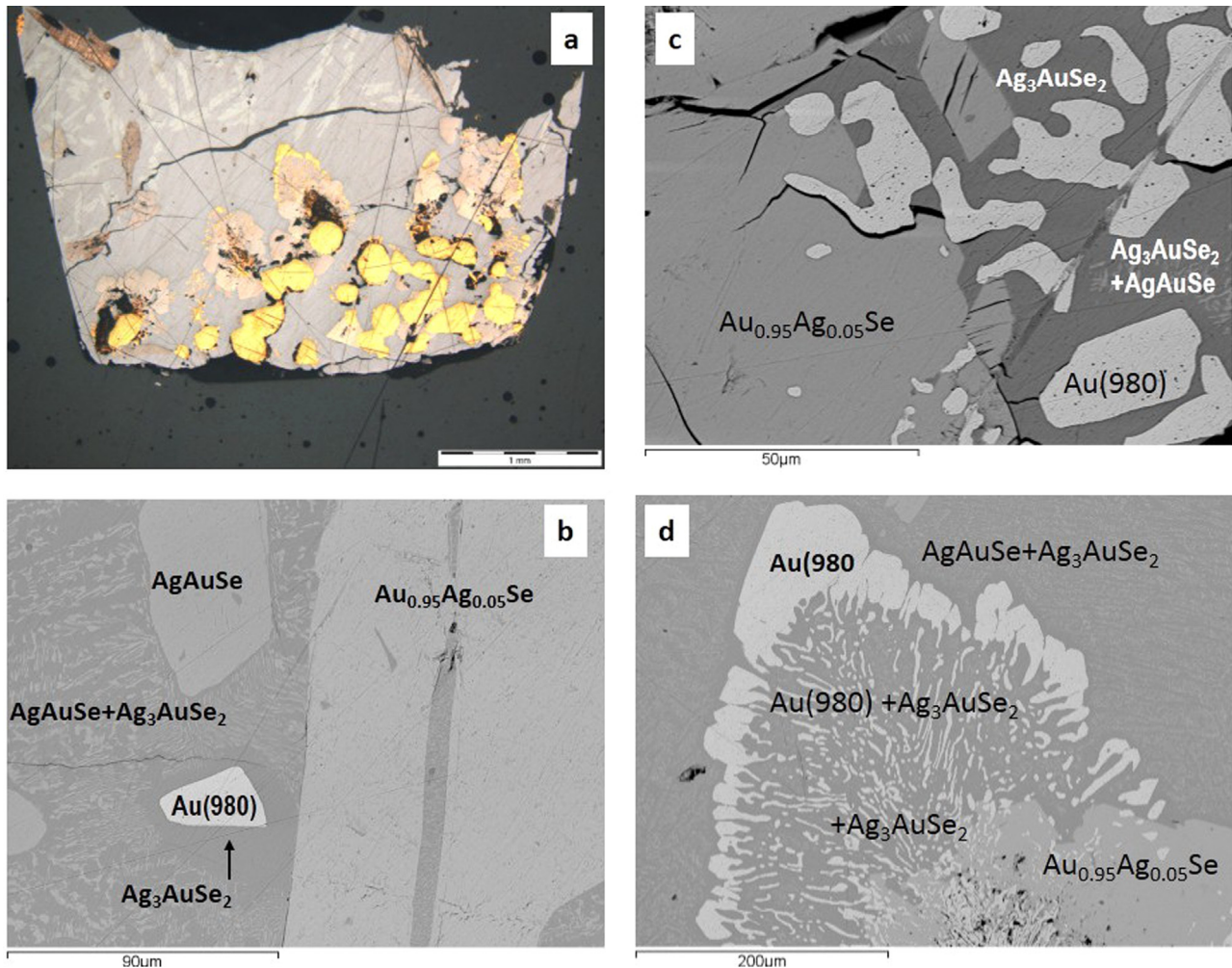


Fig. 3. Optical (a) and SEM photos (b–d) of microstructure of synthesized polyphase sample with initial composition AgAuSe (#5, Table 1).

and Au–Ag alloy 980–1000%. In the experimental sample with the initial composition $x=0.75$ no Au–Ag alloy was detected.

SEM photos of polished fragments of four polyphase samples from the experiments with $x=0.25, 0.75, 1.25$ and 1.75 (#2, 4, 6, 8, Table 1) are shown in Fig. 2(a–d). Fig. 2(a) shows acanthite–fischesserite intergrowths arranged between rounded grains of Au–Ag alloy. Selenides of Ag_3AuSe_2 and AgAuSe compositions also form intergrowths (Fig. 2(c,d)). Moreover, AgAuSe also occurs rather large leaf-shaped grains (Fig. 2(b,c); Fig. 3(b)). Selenide AuSe forms separate grains up to $40\text{--}50\ \mu\text{m}$ or their aggregates. The grains of Au–Ag alloys in the synthesized products have mainly a rounded or oval shape.

Fig. 3a shows a photograph of a polished fragment of the ingot with $x=1$ (AgAuSe) (#5, Table 1). One can see from these photo the amount of petroskaite-like phase is 20–30 rel.%. Fig. 3(b–d) demonstrate the detailed relationships of phases in the ingot. Unlike the experiments with $x=0.75$ and 1.25 (#4 and 6, Table 1; Fig. 2(c,b)) gold forms mirmekite-like intergrowths with fischesserite and microinclusions in gold selenide (Fig. 3(d)). It is worth noting that in all the experiments selenium was present on the walls of the ampoules in minor amounts in the form of black micro hemispheres, except the experiment with the initial composition Au_2Se .

Fig. 4 shows the X-ray powder diffraction patterns of synthesized samples with bulk composition $\text{Ag}_{2-x}\text{Au}_x\text{Se}$ ($x=0.25; 0.75; 1.25; 1.5; 1.75$) (#2, 4, 6–8, Table 1). The sample with $x=0.25$ is a

mixture of naumannite and fischesserite. The profiles of other samples display peaks of fischesserite Ag_3AuSe_2 and $\beta\text{-AuSe}$ (card 04-004-4751). As the fraction of gold in the total composition of sample increases, the content of fischesserite decreases with the proportional growth of AuSe concentration. The sample with $x=1.75$ in addition to AuSe and fischesserite also contains a metallic phase (Au, Ag or their alloy). Results of microprobe analysis show that a phase of AgAuSe composition is present in five experiments (#4–8, Table 1). At the same time, weak peaks that can be attributed to the petroskaite-like phase are present only in the diffraction profile of the sample of AgAuSe composition (#5, Table 1). Its estimated concentration was 3%, i.e. even if this phase is present in the sample, its amount is negligible. In Fig. 5 one can see the diffraction profile of this sample compared to the diffraction patterns of petroskaite AgAuS (at the bottom) and fischesserite Ag_3AuSe_2 (at the top), and the arrows show the diffraction peaks of the petroskaite-like phase. Additional advanced study revealed that the concentration of the petroskaite-like phase of AgAuSe composition to a large degree depends on its quenching conditions [17]. Unit cell parameters of the identified phases in samples #2–8 are summarized in Table 2.

Study of the phase relationships and microstructure of synthesized samples allowed us to improve the ternary diagram of the system Ag–Au–Se (Fig. 6). This diagram in contrast to the diagrams from [9–11] at $25\text{--}227\ ^\circ\text{C}$ includes the additional phase AgAuSe and shows the existence domains of three solid solutions $\text{Ag}_2\text{Se} - \text{Ag}_{1.94}\text{Au}_{0.06}\text{Se}$,

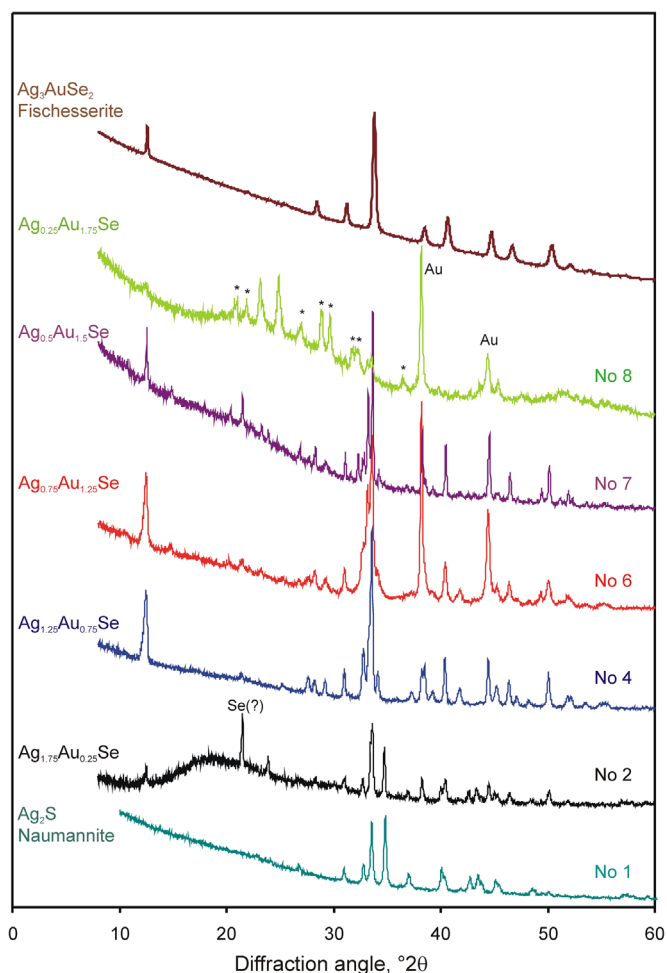


Fig. 4. Diffraction profiles of experimental samples with the initial composition $\text{Ag}_{2-x}\text{Au}_x\text{Se}$ ($x=0.25; 0.75; 1.25; 1.5; 1.75$) (#2,4,6–8, Table 1) compared to the profiles of naumannite Ag_2Se (at the bottom) and fischesserite Ag_3AuSe_2 (at the top). Profile for 8 shows the peaks of metallic phase (Au), peaks of AuSe (*), and peaks of unidentified (unknown) phase.

$\text{Ag}_{3.2}\text{Au}_{0.8}\text{Se}_2$ - Ag_3AuSe_2 and $\text{Au}_{0.94}\text{Ag}_{0.06}\text{Se}$ - AuSe.

We analyzed isomorphism of Ag–Au in synthesized phases from the viewpoint of their structural features. Cubic fischesserite structure Ag_3AuSe_2 [2], space group $I4_132$, contains triatomic linear Se–Au–Se groups and Ag atoms surrounded by four Se atoms. The coordination formula (in the formal ionic representation) is $\text{Ag}_3^{[4]}\text{Au}^{[2]}\text{S}_2^{(7)}$ where the coordination number of the cations is enclosed in brackets and that of the anions in parentheses. Fig. 7a shows a fragment of fischesserite structure: arrangement of Se–Au–Se triads on the 3-fold symmetry axis surrounded by 12 Ag atoms. Noteworthy are the unexpected features of crystal structures of fischesserite and its synthetic selenide-sulfide analogs $\text{Ag}_3\text{Au}(\text{Se}_{1.5}\text{S}_{0.5})$ and $\text{Ag}_3\text{Au}(\text{SeS})$ [15]. As typical distances are $\text{Au}^{[2]}\text{–S}$ 2.3 Å and $\text{Au}^{[2]}\text{–Se}$ 2.4 Å, falling outside these limits of “mixed” distances $\text{Au}^{[2]}\text{–}(\text{Se}_{0.5}\text{S}_{0.5})$ 2.43 Å and $\text{Au}^{[2]}\text{–}(\text{Se}_{0.75}\text{S}_{0.25})$ 2.45 Å [15] reflects the certain extension of triads (Se,S)–Au–(Se,S) in the structural type of fischesserite. In fischesserite itself, $\text{Au}^{[2]}\text{–Se}$ distance is stretched to 2.60 Å [2]. Most likely, this seems to be due to the shortening of Au–Ag and Ag–Ag distances in the surrounding of triads: with 3.05 Å in sulfide-selenides to 2.95 Å in selenide. Shortened distance Se–Se between triads in fischesserite

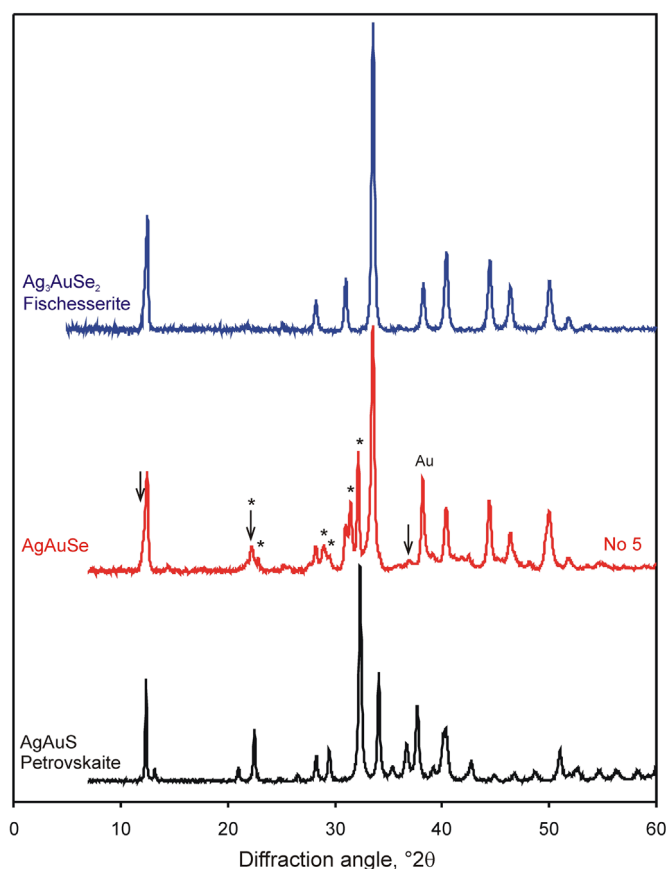


Fig. 5. Diffraction profile of experimental sample with the initial composition AgAuSe (#5, Table 1) compared to petrovskaitite AgAuS and fischesserite Ag_3AuSe_2 . The arrows show the positions of weak peaks attributed to petrovskaitite-like phase AgAuSe , the stars show the peaks of AuSe phase (card 04-004-4751).

structure 3.43 Å is also typical. This can be interpreted as expressing covalence trend of anion–anion interaction [18]. The above analysis explains why Ag easily enters the extended triad Se–Au–Se in fischesserite: the Ag–Se distances are typically longer than the Au–Se distances.

Monoclinic structure of $\beta\text{-AuSe}$ [19], space group $C2/m$, is presented in Fig. 7(b). It contains Au^+ and Au^{3+} . Au^{3+} is surrounded by four Se atoms in the form of a planar square, Au^+ is coordinated to two Se atoms. The occurrence Ag is only probable in position $\text{Au}^{[2]}$. In the Se– $\text{Au}^{[2]}$ –Se triad, distances Au–Se are 2.43 Å and Se–Au–Se angle is 180°. When Au is replaced by Ag, distances Ag–Se will tend to increase, resulting in a displacement of cation from a particular position and, hence, a decrease in Se–Ag–Se angle (at Ag–Se=2.47 Å, Se–Ag–Se angle is estimated to be 160°). This effect will cause structural tension, which explains the limited isomorphism Ag→Au.

In orthorhombic naumannite structure [20], Ag_2Se , space group $P2_12_12_1$, one Ag atom is surrounded by four Se atoms in a distorted tetrahedral coordination, while the second Ag atom exhibits a coordination defined by three Se atoms, forming a trigonal plane. Fig. 7c (at the top) illustrates a fragment of structure: four AgSe_4 -tetrahedra and three AgSe_3 -triangles around common Se. Isomorphous occurrence of Au is only probable in the position of $\text{Ag}^{[3]}$. However, the distances Ag–Se 2.65, 2.76 and 2.80 Å (average 2.74 Å) are too long for Au–Se. Therefore, Au replacing Ag must

Table 2.
Unit-cell parameters and concentrations of phases in samples #2–8.

Sample [*]	Charge composition	Space group	Type ^{**}	<i>a</i> (Å)	<i>b</i> (Å)	<i>c</i> (Å)	β (deg)	<i>V</i> (Å ³)	Phase concentration, %
2	Ag _{1.75} Au _{0.25} Se	<i>I</i> 4 ₁ 32	1	9.9595(8)				887.9(2)	30
3	Ag _{1.50} Au _{0.50} Se Ag ₃ AuSe ₂ -fichessirite	<i>P</i> 2 ₁ 2 ₁ 2 ₁	2	4.333(2)	7.051(6)	7.744(7)		236.6(2)	70
		<i>I</i> 4 ₁ 32	1	9.96446(12)				989.38(4)	100
4	Ag _{1.25} Au _{0.75} Se	<i>I</i> 4 ₁ 32	1	9.9679(6)				990.40(19)	30
		<i>P</i> 2 ₁ 2 ₁ 2 ₁	2	4.449(3)	6.948(4)	7.933(5)		245.21(18)	50
		<i>C</i> 2/ <i>m</i>	3	8.259(8)	3.627(3)	6.179(13)	106.78(7)	177.2(4)	20
5	AgAuSe	<i>I</i> 4 ₁ 32	1	9.9863(3)				995.90(8)	35
		<i>R</i> 3̄ <i>m</i>	4	13.815(3)		9.282(4)		1534.2(6)	< 5
		<i>C</i> 2/ <i>m</i>	3	8.3197(15)	3.6641(6)	6.3200(15)	106.762(14)	184.48(4)	60
6	Ag _{0.75} Au _{1.25} Se	<i>I</i> 4 ₁ 32	1	9.9652(7)				989.6(2)	25
		<i>C</i> 2/ <i>m</i>	3	8.514(12)	3.439(5)	6.080(9)	104.09(13)	172.7(3)	75
		<i>C</i> 2/ <i>m</i>	3	8.267(5)	3.609(2)	6.668(4)	105.75(5)	983.49(6)	35
7	Ag _{0.50} Au _{1.50} Se	<i>I</i> 4 ₁ 32	1	9.9447(2)				182.00(11)	65
		<i>C</i> 2/ <i>m</i>	3	8.267(5)	3.609(2)	6.668(4)	105.75(5)	988.8(18)	5
		<i>C</i> 2/ <i>m</i>	3	8.3359(17)	3.6299(8)	6.6439(14)	106.048(17)	193.20(4)	75
8	Ag _{0.25} Au _{1.75} Se	<i>I</i> 4 ₁ 32	1	9.963(6)				67.576(19)	20
		<i>Fm</i> 3̄ <i>m</i>	5	4.0731(4)					

^{*} Samples are numbered according to Table 1.

^{**} 1- petzite type, 2 – naumannite type, 3 – β-AuS type, 4 – petrovskaita type, 5 – metal (Au) phase.

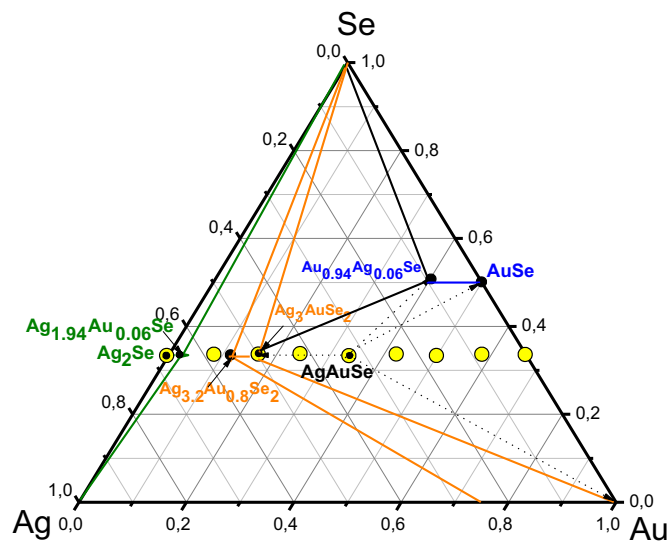


Fig. 6. The phase diagram of Ag-Au-Se at 500 °C based on the results of experiments with initial composition Ag_{2-x}Au_xSe (*x*=0; 0.25; 0.5; 0.75; 1; 1.25; 1.5; 1.75; 2) and literature data from [9–11].

lose one bond with Se for stable configuration, shifting to one of the triangle edges. But shifting is prevented by the surrounding of Ag^[3] position by other metal atoms (at distances of about 3.0 – 3.3 Å, Fig. 7c). As a result, Au^[2+1]→Ag^[3] replacement does not exceed several percents.

Results of our studies prove the existence of a series of natural solid solutions among Ag-Au selenides: Au-bearing naumannites and Ag-rich fischesserites. The electron microprobe analysis data of these minerals known from literature data confirm the presence of Au impurity in naumannites [21] and a higher Ag content in fischesserites [4,21,22]. The selenide assemblages form in nature at temperatures substantially below those of our experiments. However, recent studies of epithermal gold-silver-selenide (telluride) systems have shown that many of them are part of a

broader magmatic-epithermal system [3], which suggests higher temperatures and possible involvement of the melts at the early stages of mineralization.

4. Conclusions

1. Limited isomorphism Ag ↔ Au was established in selenides: Ag₂Se – Ag_{1.94}Au_{0.06}Se, Ag₃AuSe₂ – Ag_{3.2}Au_{0.8}Se₂ and AuSe – Au_{0.94}Ag_{0.06}Se.
2. New phases – three solid solutions and petrovskaita-like phase of AgAuSe were introduced to the phase diagram of Ag-Au-Se.
3. Ag-Au isomorphism in selenides is limited by structural features

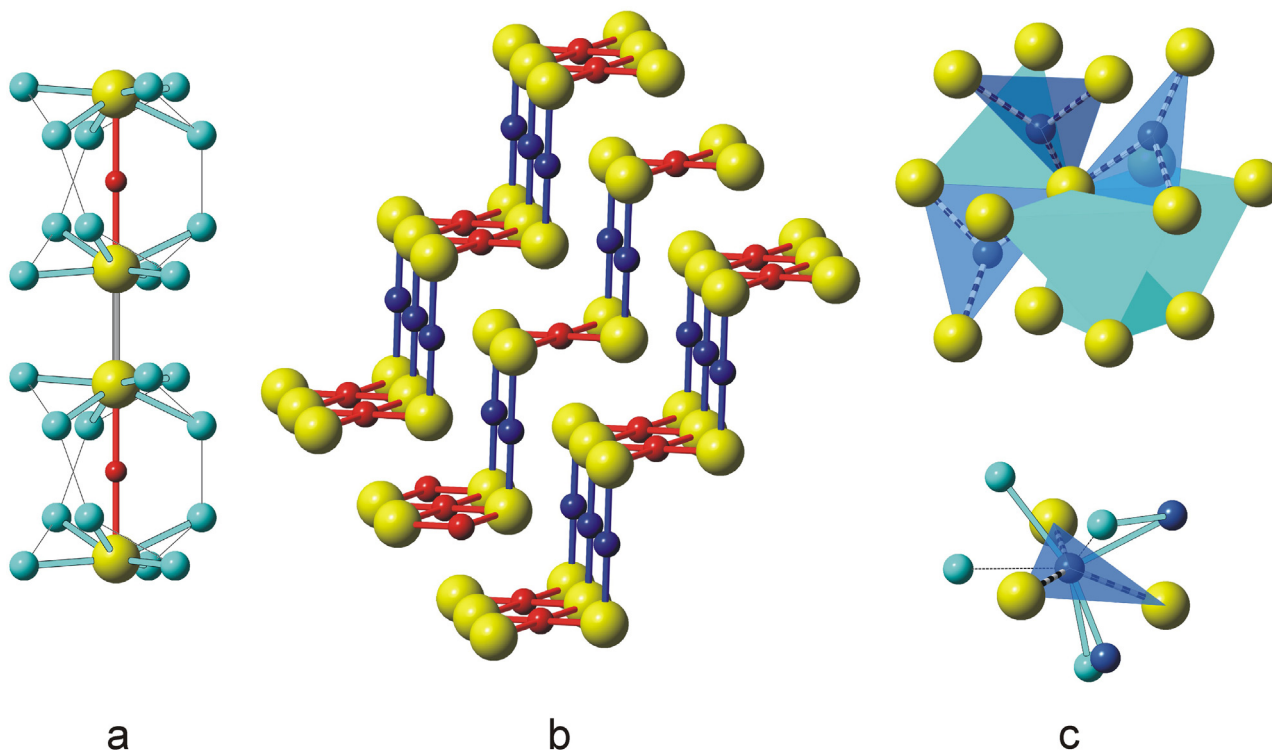


Fig. 7. a) A fragment of structure of fischerite Ag_3AuSe_2 ; b) Structure of $\beta\text{-AuSe}$, projection \sim along axis b ; c) Two fragments of structure of naumannite Ag_2Se : at the top – 4 AgSe_4 -tetrahedra and 3 AgSe_3 -triangles around common Se; at the bottom – surrounding of Ag^{3+} position by six Ag^{4+} and Ag^{3+} at distance of about 3.0 – 3.3 Å.

of fischerite, naumannite, and AuSe.

4. Contents of gold in selenium and selenium in gold are below the detection limit of microprobe analysis.

Acknowledgments

This work is supported by Integration project N48 from the Siberian Branch of the Russian Academy of Sciences. Authors are grateful to Dr. N.S. Karmanov (Institute of Geology and Mineralogy SB RAS) for electron microprobe data. We would like to express our sincere thanks to the editor and anonymous reviewer for their comments and suggestions.

References

- [1] A.M. Evans, *Ore Geology and Industrial Minerals* (3rd ed.), Blackwell, London, 1993.
- [2] L. Bindi, C. Cipriani, *Can. Miner.* 42 (2004) 1733.
- [3] C.L. Ciobanu, N.J. Cook, P.G. Spry, *Miner. Pet.* 87 (2006) 163.
- [4] E.M. Spiridonov, S.V. Filimonov, I.A. Bryzgalov, *Dokl. Earth Sci.* 425A (2009) 415.
- [5] G.E. Cranton, R.D. Heyding, *Can. J. Chem.* 46 (1968) 2637.
- [6] M.D. Barton, *Econ. Geol.* 75 (1980) 303.
- [7] Yu.V. Seryotkin, V.V. Bakakin, G.A. Pal'yanova, K.A. Kokh, *CrystEngComm* 16 (2014) 1675.
- [8] Yu. V. Seryotkin, V.V. Bakakin, G.A. Pal'yanova, K.A. Kokh, *Cryst. Growth Des.* 11 (2011) 1062.
- [9] G.A. Wiegers, *J. Less-Common Met.* 48 (1976) 269.
- [10] E.G. Osadchii, E.A. Echmaeva, *Am. Miner.* 92 (2007) 640.
- [11] D. Feng, P. Taskinen, *J. Alloy. Compd.* 583 (2014) 176.
- [12] I.Ya. Nekrasov, S.E. Lunin, L.N. Egorova, *Dokl. Akad. Nauk.*, 311 (4), 1990, p. 943.
- [13] K. Soldenhoff, Patent US 20110083531 A1 20.04.2011.
- [14] G.A. Pal'yanova, K.A. Kokh, Yu.V. Seryotkin, *Russ. Geol. Geophys.* 52 (2011) 443.
- [15] Yu.V. Seryotkin, G.A. Pal'yanova, V.V. Bakakin, K.A. Kokh, *Phys. Chem. Miner.* 40 (2013) 229.
- [16] A.C. Larson, R.B. von Dreele, General structure analysis system, Los Alamos National Laboratory Report, 2000, p. 86.
- [17] G.A. Palyanova, Yu.V. Seryotkin, V.V. Bakakin, K.A. Kokh, *J. Alloy. Compd.* 664 (2016) 385.
- [18] E. Makovicky, *Rev. Mineral. Geochem.* 61 (2006) 7.
- [19] A. Rabenau, H. Schulz, *J. Less-Common Met.* 48 (1976) 89.
- [20] J. Yu, H. Yun, *Acta Crystallogr.* E67 (2011) 45.
- [21] H.A. Cocker, J.L. Mauk, S.D.C. Rabone, *Miner. Depos.* 48 (2013) 249.
- [22] Mineral Data Publishing, 2001–2005, version 1, Fischerite (<http://www.zpag.net/Mineraux/PDF/fischerite.pdf>).